



# Copper transport and sulphide sequestration during copper corrosion in anaerobic aqueous sulphide solutions

J. Chen\*, Z. Qin, T. Martino, M. Guo, D.W. Shoesmith\*

Department of Chemistry and Surface Science Western, University of Western Ontario, London, Ontario, N6A 5B7, Canada



## ARTICLE INFO

### Keywords:

- A. Copper
- B. SEM
- C. Interfaces

## ABSTRACT

The corrosion of copper in aqueous solutions containing  $\geq 5 \times 10^{-4}$  mol/L sulphide and the ensuing accumulation of corrosion product deposits (as chalcocite  $\text{Cu}_2\text{S}$ ) occurs non-uniformly indicating the occurrence of microgalvanic coupling between net anodic and net cathodic surface locations. A series of novel electrochemical experiments were designed to confirm the occurrence of this process and a series of analytical procedures used to identify the chemical nature of the transported Cu species. Transport was found to occur as copper sulphide complexes and clusters. It was also demonstrated that all the available sulphide was sequestered as deposited  $\text{Cu}_2\text{S}$ .

## 1. Introduction

The combination of mass transport and electrochemical/chemical reactions [1] is important in a range of processes such as mineral growth [2–5], mineral nutrient adsorption/digestion [6–9] and film deposition [10–13]. The reaction paths and rates of such processes are commonly dependent on the nature of the transported species which are often difficult to define. The transport of trace metals (such as Cu, Fe and Zn) in natural environments in the form of either organic sulphide complexes [14] or inorganic sulphide clusters [15] is a potential source of toxicity. This transportability of organic sulphide complexes has been utilized to grow chalcocite ( $\alpha\text{-Cu}_2\text{S}$ ) films using aerosol-assisted chemical vapour deposition [16].

When present in aqueous solutions sulphide destabilizes metals such as Cu leading to corrosion and the deposition of sulphide films (chalcocite) [17–28]. Depending on the exposure conditions the distribution of sulphide films on corroding Cu surfaces can be non-uniform. Previously, it has already been shown that areas covered with a relatively thin  $\text{Cu}_2\text{S}$  film acted as net anodes galvanically-coupled to areas covered with a thicker film acting as a net cathode [13], and that this galvanic couple involved the transport of Cu from anodes to cathodes. However, the transportable species was not identified.

A knowledge of transportable species is important to understand a series of processes including mineralization, the control of sulphide film growth for photovoltaics, and the corrosion of high-level nuclear waste containers in Sweden, Finland and Canada [29–31]. Given that waste containment is required for many thousands of years, the last application is of particular interest.

In previous experiments [13], we have confirmed that microgalvanic coupling of local anodes and cathodes can occur when  $[\text{SH}^-] \geq 5 \times 10^{-4}$  mol/L. In one of these experiments a potential cathode was prepared by exposing a Cu electrode to a 0.1 mol/L NaCl solution containing  $5 \times 10^{-4}$  mol/L  $\text{Na}_2\text{S}$  for 1211 h. This electrode was then re-immersed in the same solution for a further 480 h galvanically-coupled to an uncorroded Cu specimen (for a total immersion period of 1691 h). This arrangement mimicked the microgalvanic coupling of areas covered by a thick  $\text{Cu}_2\text{S}$  deposit, and hence potential cathodes, with exposed Cu areas which could then act as preferential anodes. The film formed on the potential cathode was 2–4  $\mu\text{m}$  thick compared to that formed on an uncoupled electrode exposed for the same period (1691 h) which was  $\sim 700$  nm thick.

That the separated electrodes were galvanically coupled was confirmed electrochemically, a coupled current density of  $\sim 0.1 \mu\text{A}/\text{cm}^2$  and a coupled potential of  $\sim 2\text{--}6$  mV being measured with the pre-corroded specimen acting as the net cathode. Analysis of the solution on completion of the experiment detected 11  $\mu\text{g}/\text{L}$  of dissolved Cu confirming the presence of transportable species. While microgalvanic coupling was still occurring on the individual electrodes, this experiment confirmed the occurrence of macrogalvanic coupling (i.e., the coupling between the separated electrodes as opposed to microgalvanic coupling between sites on the same electrode) with the thickened film on the net cathode suggesting accumulation of Cu transported from the net anode [13].

Despite this demonstration that galvanic coupling between separated locations on a corroding surface could occur, this experiment did not confirm that the accumulation of a thick deposit involved the

\* Corresponding authors.

E-mail addresses: [jchen496@uwo.ca](mailto:jchen496@uwo.ca) (J. Chen), [dwsheosm@uwo.ca](mailto:dwsheosm@uwo.ca) (D.W. Shoesmith).

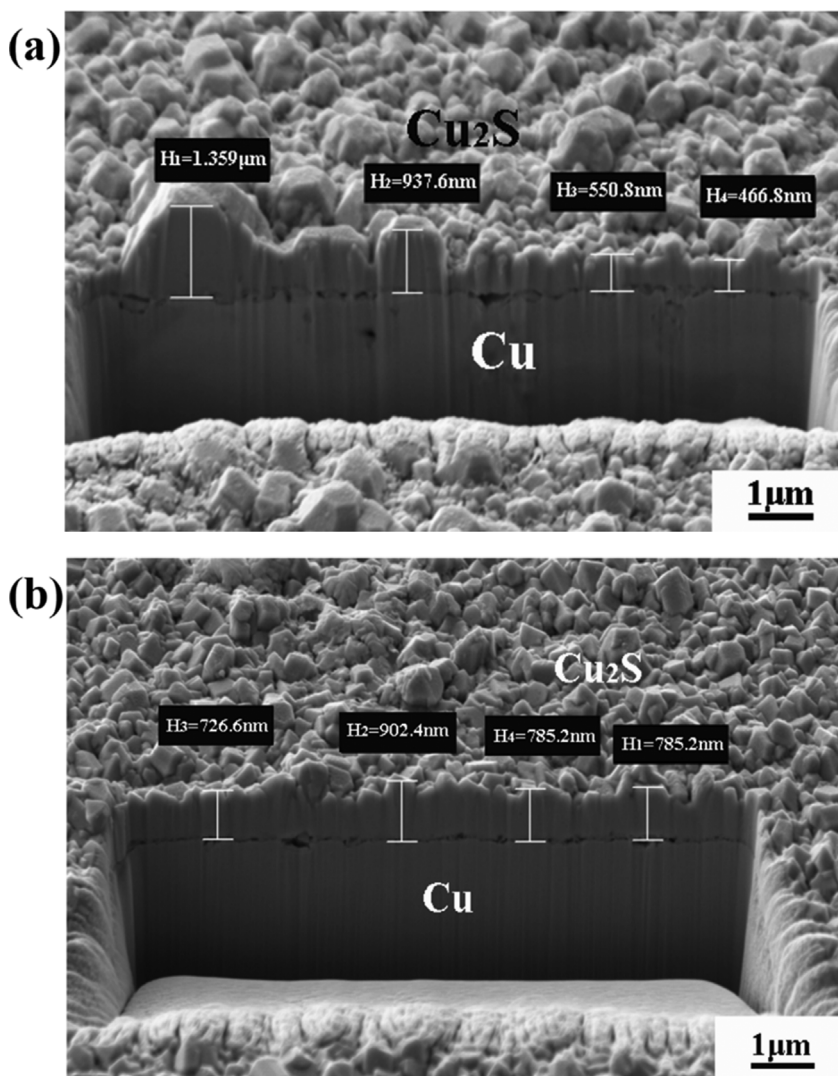


Fig 1. FIB cut cross sections of (a) the net cathode in experiment 1 after 1691 h immersion in 0.1 mol/L NaCl +  $5 \times 10^{-4}$  mol/L  $\text{SH}^-$  solution, and (b) the net anode after the final 480 h immersion in the same solution.

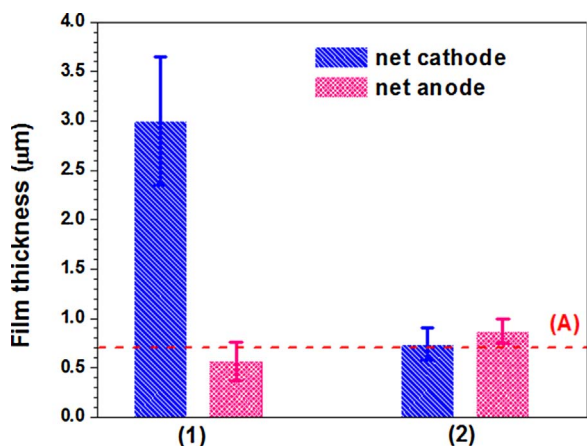


Fig. 2. The thickness of the sulphide film formed on the net cathodes and net anodes after exposure in sulphide solutions. (1) Net cathodes and net anodes with Cu transport between them [13]; and (2) Net cathodes and net anodes without Cu transport between them. The red dashed line (A) represents the average film thickness measured on a specimen not galvanically coupled. (For interpretation of the references to colour in this figure legend, the reader is referred to the web version of this article.)

transport of Cu species between coupled anodes and cathodes, and, if it did, what the nature of the transported species was. In this paper we confirm that galvanic coupling does involve transport of Cu from

Table 1  
ICP-MS analyses of the dissolved and total Cu contents in the solution from experiment 3.

Sample	Cu content (μg/L)	Detect limit (μg/L)
dissolved metal	15.5	2
total metal	34	5

anodes to cathodes and identify the transportable species involved. All experiments were performed in an Ar-purged anaerobic chamber to avoid sulphide oxidation. To ensure consistency with previous studies all experiments have been conducted in a 0.1 mol/L NaCl solution containing  $5 \times 10^{-4}$  mol/L  $\text{Na}_2\text{S}$ .

## 2. Materials and methods

Experiments were conducted using P-doped (30–100 ppm), O-free copper (Cu-OF) provided by the Swedish Nuclear Fuel and Waste Management Co. (SKB), Stockholm. Cu disk working electrodes (1 cm in diameter) were cut from plate material. The disks were connected to a stainless steel shaft and painted with a non-conductive lacquer to prevent contact of the Cu/steel junction with the solution. The electrodes were then heated (60 °C for 12 h) to promote adhesion of the paint. The exposed flat surface was ground successively with 240, 600, 800, 1000, 1200 grade SiC paper, then polished to a mirror finish using 1 μm, 0.3 μm, and, finally, 0.05 μm  $\text{Al}_2\text{O}_3$  suspensions. Prior to

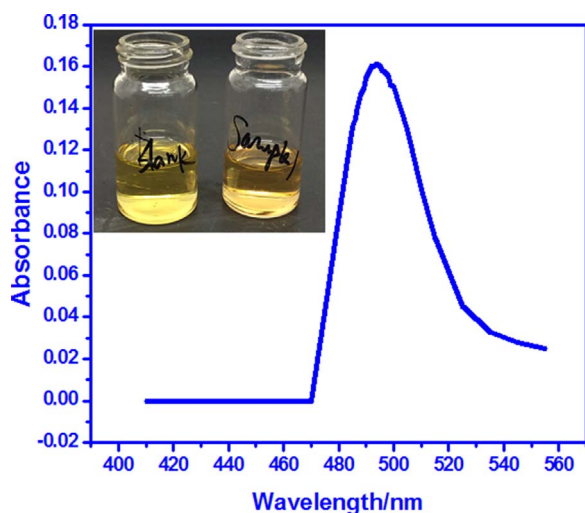


Fig. 3. UV spectrum of the solution from experiment 3. The insert shows the color difference between the background (blank) and experimental (sample) solutions.

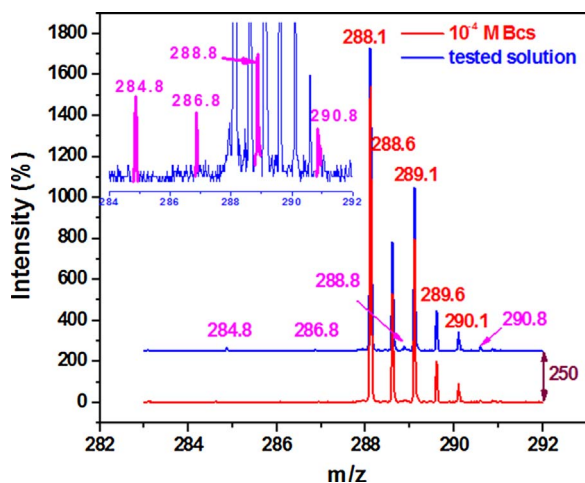


Fig. 4. Mass spectrum of a solution sample from experiment 3 compared to a background spectrum. The insert shows the characteristic peaks (pink) for the  $\text{Cu}_3\text{S}_3$  cluster. The blue spectra was shifted 250 intensity units in Fig. 4. (For interpretation of the references to colour in this figure legend, the reader is referred to the web version of this article.)

experiments, electrodes were washed with Type I water (resistivity = 18.2 M $\Omega$  cm, obtained from a Thermo Scientific Barnstead Nanopure 7143 ultrapure water system), ultrasonically cleaned using methanol (reagent grade), washed with Type I water, and dried using ultra-pure Ar.

To ensure anoxic conditions, experiments were performed in an Ar-purged anaerobic chamber (Canadian Vacuum Systems Ltd.), maintained at a positive pressure (2–4 mbar) by an MBraun glove box control system. The oxygen concentration in the chamber was analyzed with an MBraun oxygen probe with a detection limit of 1.4 mg/m<sup>3</sup>. The anaerobic chamber was maintained at a total oxygen concentration  $\leq$  4.2 mg/m<sup>3</sup>, which includes the oxygen in both air and vapor. The actual oxygen content of the solution should be less than this value. Even though there is a trace amount of oxygen present, copper sulphide is more stable in sulphide solution than copper oxide based on thermodynamic data ( $\Delta G^\circ = -101.46$  kJ/mol for the conversion from  $\text{Cu}_2\text{O}$  to  $\text{Cu}_2\text{S}$  in sulphide solutions at 298 K [32]:  $\text{Cu}_2\text{O}(\text{s}) + \text{HS}^-(\text{aq}) \rightarrow \text{Cu}_2\text{S}(\text{s}) + \text{OH}^-(\text{aq})$ ) and available literature [33–36].

The 0.1 mol/L NaCl +  $5 \times 10^{-4}$  mol/L  $\text{Na}_2\text{S}$  solution was prepared with Type I water, reagent-grade sodium sulphide ( $\text{Na}_2\text{S} \cdot 9\text{H}_2\text{O}$ , 98.0% assay) and sodium chloride (NaCl, 99.0% assay), to simulate the saline groundwater conditions anticipated in a high level nuclear waste

repository. The 0.1 mol/L  $\text{Na}_2\text{SO}_4$  solution was prepared with Type I water and reagent-grade sodium sulphate ( $\text{Na}_2\text{SO}_4$ , 100.1% assay). The bathocuproine disulfonate (Bcs) solutions were prepared with Type I water and bathocupronedisulfonic acid disodium salt purchased from Sigma-Aldrich Co.

Electrodes were immersed in the sulphide solutions for various exposure periods. A standard three-electrode cell with a Pt plate counter electrode and a saturated calomel reference electrode (SCE) was used. Prior to each experiment, electrodes were cathodically cleaned at  $-1.6$  V/SCE for 2 min and then at  $-1.15$  V/SCE for 2 min. Six experiments (Experiment 1–6) were carried out either under natural corrosion conditions or under galvanically polarized conditions to confirm the Cu transport phenomenon, to identify the transportable Cu species and to determine the Cu transport mechanism. The experimental details of each experiment are described below.

Since exposure periods were long, the  $[\text{SH}^-]$  was monitored weekly by measuring the pH as described previously [17] and  $\text{SH}^-$  added to readjust the  $[\text{SH}^-]$  to its original value. Experiments were performed at  $25 \pm 2$  °C. Electrodes removed from solution for surface analyses were rinsed with Type I water for 10 min and dried with cold Ar gas. Analyses were then performed after a minimum period of interim storage ( $< 30$  min). The surface and cross-sectional morphologies of corroded specimens were observed using a Leo 1540 scanning electron microscope (SEM) equipped with a focused ion beam (FIB) (Zeiss Nano Technology Systems Division, Germany). The composition of films was qualitatively analyzed by energy dispersive X-ray spectroscopy (EDS) using a Leo 1540 FIB/SEM microscope (the oxygen detection limit is 1 at.%). Mass spectrometry (MS) analysis was performed using a Bruker MicroTOF 11 mass spectrometer in a negative-ion mode. The Cu content of solutions was analyzed using inductively coupled plasma mass spectrometry (ICP-MS).

### 3. Results and discussion

#### 3.1. Evidence for Cu transport

In experiment 1, a Cu electrode with a diameter of 1 cm was pre-corroded in an electrochemical cell for 1211 h. This electrode was then galvanically-coupled to an uncorroded Cu electrode located in a second electrochemical cell, with the two cells connected through a KCl-saturated agar salt bridge. The experiment was then continued for a further 480 h for a total immersion time of 1691 h. With one exception, this experiment was identical in all aspects to that discussed above, and described in reference 13. As opposed to the previous experiment, while the pre-corroded electrode can act as a net cathode and the uncorroded electrode as a net anode the transport of Cu between them is precluded by the use of the salt bridge.

That these electrodes were galvanically coupled was demonstrated electrochemically. The potential difference between the two electrodes was 2–6 mV and the current density  $\sim 0.1$   $\mu\text{A}/\text{cm}^2$  with the pre-corroded electrode functioning as the net cathode, and the originally uncorroded electrode as the net anode. Fig. 1 shows the FIB-cut cross sections of the net cathode and net anode. The surface of the net cathode was covered with a compact crystalline film, Fig. 1(a), with an average thickness of  $\sim 740$  nm. This was very similar to the thickness of the film grown on a Cu specimen exposed for the full immersion period, but not galvanically coupled and considerably lower than that observed in the previous galvanically-coupled experiment [13], as shown in Fig. 2. A similarly crystalline deposit was observed on the net anode, Fig. 1(b), with a thickness between 800 and 900 nm which is approximately twice as thick as that observed in the previous galvanically-coupled experiment [13], Fig. 2. Due to the blocking effect of the agar salt bridge on Cu transport, the anodic dissolution of the net anode polarized by the net cathode led to Cu deposition on its surface, which would account for  $\sim 850$  nm thick sulphide film on the net anode according to galvanic current density in Ref. 13. Consequently, the

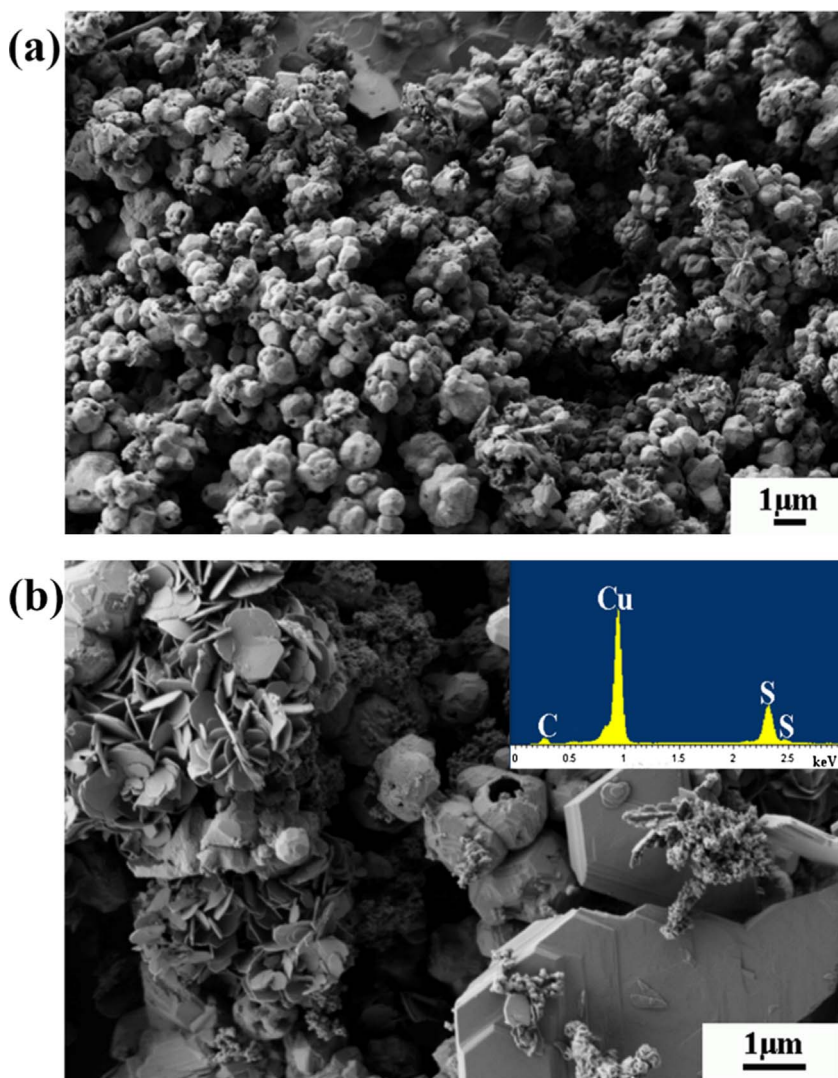


Fig. 5. (a) and (b) SEM micrographs of copper sulphide deposited with different sizes after the addition of a sulphide solution to the  $\text{CuCl}_2^-$  solution prepared in experiment 4. The insert in Fig. 5(b) shows the EDS spectrum confirming the deposition of  $\text{Cu}_2\text{S}$ .

sulphide film formed on the net anode was thicker than that on the net cathode, Fig. 1.

This rebalancing of accumulated  $\text{Cu}_2\text{S}$  deposits confirmed that, while microgalvanic corrosion could continue on the net cathode since the cathodic protection provided by the coupled net anode was weak, no large accumulation of  $\text{Cu}_2\text{S}$  could occur in the absence of a transport path for Cu species in the present experiment. These observations clearly demonstrated that the very thick film accumulated on the net cathode in the previous experiment [13], Fig. 2, could be attributed to Cu transport from the net anode.

### 3.2. Determination of the transported Cu species

In anaerobic sulphide solutions, a number of species including  $\text{Cu}^+$ ,  $\text{CuCl}_2^-$ , copper sulphide complexes [37,38] and clusters [15] could be responsible for the transport of Cu.

#### 3.2.1. Transport as $\text{Cu}^+$

Experiment 2 was similar to experiment 1. In Experiment 2, both the net anode and net cathode (pre-corroded for 1211 h in 0.1 mol/L NaCl +  $5 \times 10^{-4}$  mol/L  $\text{Na}_2\text{S}$  solution) were placed and connected in the same electrochemical cell without a salt bridge, but with a Pt electrode included in the cell during the final 480 h immersion period when the net cathode was galvanically-connected to the net anode. The distance between the net cathode and net anode was 5 cm. The Pt electrode with

a surface area of  $9 \text{ cm}^2$  was placed between the net anode and net cathode, i.e., in the transport pathway between them, and galvanostatically polarized at a current density of  $0.1 \mu\text{A}/\text{cm}^2$ . On completion of the experiment after 1691 h the Pt electrode was removed and examined by SEM and EDS. No films were detected on the Pt surface confirming that  $\text{Cu}^+$  was not the species responsible for Cu transport from the net anode to the net cathode. This experiment is further interpreted below in the light of subsequent results.

#### 3.2.2. Transport as Cu sulphide complexes

Geologic studies [37,38] have shown that three Cu sulphide complexes could be present in natural environments,  $\text{CuSH}$ ,  $\text{Cu}(\text{SH})_2^-$  and  $\text{Cu}_2\text{S}(\text{SH})_2^{2-}$  and thermodynamic calculations show that the dominant complex in 0.1 mol/L NaCl containing  $5 \times 10^{-4}$  mol/L  $\text{Na}_2\text{S}$  will be  $\text{Cu}(\text{SH})_2^-$ , which presents at a concentration 7 orders of magnitude greater than the dominant chloride complex,  $\text{CuCl}_2^-$ , indicating that the  $\text{CuCl}_2^-$  content was negligible since the soluble Cu content was low (Table 1). In addition, both laboratory and natural water studies [38] using Fourier transform mass spectrometry have shown Cu and other metal cations are present in the form of clusters or particles at concentrations up to  $\sim 600 \text{ nmol}/\text{L}$  and 100–200 nm in size. The presence of these species was shown to sequester > 90% of the sulphide in natural environments.

To confirm the presence of Cu species in the solution experiment 1 was repeated (experiment 3), and after 240 h of exposure as a galvanic

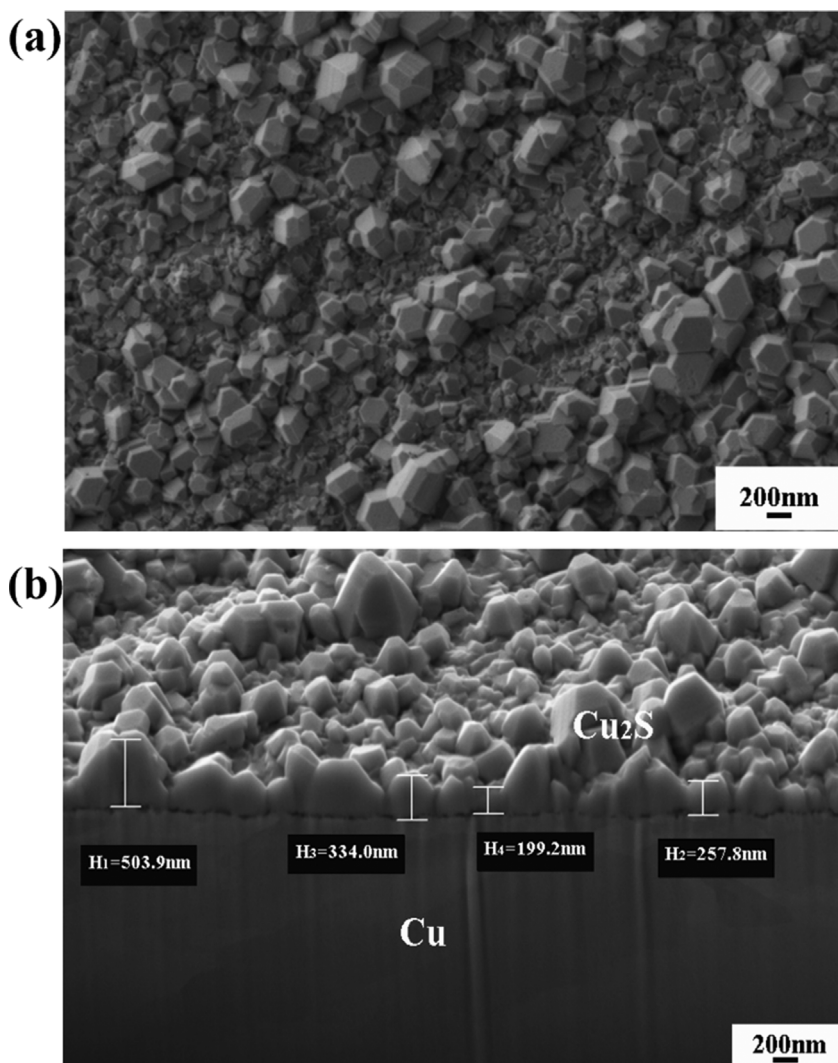


Fig. 6. (a) SEM image and (b) FIB cut cross section of the Cu electrode after 430 h immersion in the filtered solution from experiment 4.

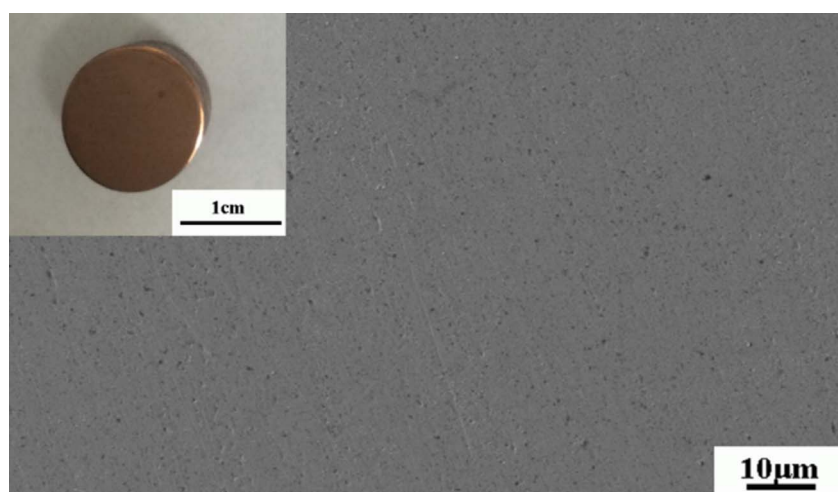


Fig. 7. SEM image of Cu sample after 430 h immersion in the 0.1 mol/L  $\text{Na}_2\text{SO}_4$  solution used in experiment 6. The inset shows the optical image of the surface.

couple (i.e., halfway through the 480 h period of galvanic coupling) bathocuproine disulfonate (Bcs), a selective chelating agent for  $\text{Cu}^+$  species [39] was added to a concentration of  $10^{-3}$  mol/L. Since the formation constant for the  $\text{Cu}^+(\text{Bcs})_2^{3-}$  complex ( $10^{19.9}$ ) is considerably larger than that of the  $\text{Cu}(\text{SH})_2^-$  complex ( $10^{17.18}$ ) and the [Bcs] was double  $[\text{SH}^-]$ , this addition would be expected to extract soluble  $\text{Cu}^+$  as  $\text{Cu}^+(\text{Bcs})_2^{3-}$ .

To confirm the identity of the complex formed after the addition of Bcs, a 3 mL sample of solution was extracted from the experimental solution for UV spectroscopic analysis. Since  $\text{Cu}^+$  species are unstable in air, 1.5 mL of a 10 wt.% solution of the reducing agent  $\text{NH}_4\text{OH}\cdot\text{HCl}$  was added to the sample, buffered with 3 mL of an  $\text{NaCH}_3\text{COO}$  solution ( $\text{pH} = 5.5$ ), to stabilize the  $\text{Cu}^+(\text{Bcs})_2^{3-}$  complex. A reference (blank) solution containing 3 mL  $10^{-3}$  mol/L Bcs, 1.5 mL of 10 wt.%

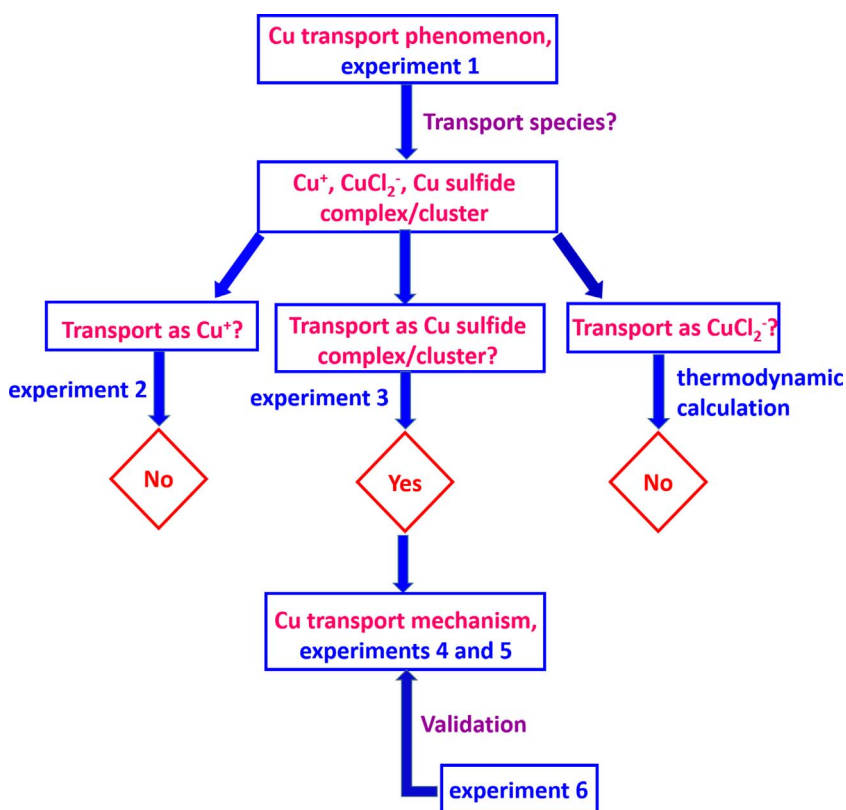


Fig. 8. Logic map for the sequence of experiments performed to investigate Cu transport and sequestration.

$\text{NH}_4\text{OH}\cdot\text{HCl}$  solution and 3 mL of  $\text{NaCH}_3\text{COO}$  solution was also prepared. The colour difference between the sample and the blank solution is shown in Fig. 3, indicating the presence of the Bcs complex in the sample. The presence of this complex was confirmed by UV spectroscopy, the absorbance peak at a wavenumber of 490 nm [39–41] confirming its presence, Fig. 3. Consistent with thermodynamic calculations this confirmed the presence of soluble  $\text{Cu}(\text{SH})_2^-$  complexes subsequently converted to  $\text{Cu}^+(\text{Bcs})_2^{3-}$  complexes in the galvanically-coupled experiment 3.

To detect whether Cu sulphide clusters were also present in the solution from the galvanically-coupled experiment (experiment 3), mass spectrometry (MS) was performed on a ten-fold diluted solution sample. Fig. 4 shows the spectra obtained on a solution sample, and on a background reference sample containing only  $10^{-4}$  mol/L of Bcs. When compared to a theoretical isotopic simulation for  $\text{Cu}_3\text{S}_3$  clusters [15], the spectrum matched the theoretical peaks except for the peak at 288.8  $m/z$ , Fig. 4. This peak was attributed to a contribution from Bcs. No evidence of the formation of  $\text{Cu}_4\text{S}_6$  clusters was observed in contrast to published claims [15]. These results confirm the presence of  $\text{Cu}_3\text{S}_3$  clusters in the galvanically-coupled experiment. Similar MS analyses were performed on the same solution without the addition of Bcs, and showed that the intensities of characteristic MS peaks were similar to those observed with the addition of Bcs. This indicates that there was no conversion between  $\text{Cu}_3\text{S}_3$  cluster and  $\text{Cu}^+(\text{Bcs})_2^{3-}$  complexes in experiment 3.

Table 1 shows that the concentration of dissolved Cu, determined by ICP-MS was 15.5  $\mu\text{g/L}$ . If  $\text{HNO}_3$  was added to redissolve the  $\text{Cu}_3\text{S}_3$  clusters, the concentration of Cu increased to 34  $\mu\text{g/L}$  confirming both complexes and clusters were present.

### 3.3. Cu transport mechanism and sulphide sequestration

While the above experiments confirm that Cu can be transported in sulphide solutions predominantly in the form of  $\text{Cu}(\text{SH})_2^-$  complexes but also in particulate form, it remains to be demonstrated that, under

the conditions when microgalvanic coupling occurred leading to the uneven distribution of corrosion (i.e., at  $[\text{SH}^-] \geq 5 \times 10^{-4}$  mol/L [13]), all the available sulphide was eventually consumed and that the extent of corrosion was limited by the amount of available sulphide. Previously we proposed that the transport of Cu from the corroding anode could be in the form  $\text{CuCl}_2^-$  since  $\text{SH}^-$  would be depleted by its consumption in the corrosion process. However, as demonstrated by thermodynamic calculations [37,38] such a species was unlikely to have persisted once the bulk solution  $[\text{SH}^-]$  was encountered, when conversion to  $\text{Cu}(\text{SH})_2^-/\text{Cu}_3\text{S}_3$  would have occurred.

The following experiments were performed to demonstrate that  $\text{Cu}(\text{SH})_2^-$  species were eventually deposited as  $\text{Cu}_2\text{S}$  in the process sequestering all the available sulphide.

In experiment 4 a saturated solution of  $\text{CuCl}_2^-$  was prepared by galvanostatically oxidizing Cu at a current of 1 mA in anoxic 0.1 mol/L NaCl for 27 h [42]. Cu dissolved in excess of the solubility limit was precipitated as CuCl. Based on the electrochemical charge consumed the amount of oxidized Cu was  $1.01 \times 10^{-3}$  moles. The Cu electrode was then removed and 0.11 g of  $\text{Na}_2\text{S}\cdot 9\text{H}_2\text{O}$  added yielding a solution with a  $[\text{SH}^-]$  of  $4.58 \times 10^{-4}$  mol/L. Since the formation constant of  $\text{CuCl}_2^-$  ( $3 \times 10^5$ ) [43] is much lower than that of  $\text{Cu}(\text{SH})_2^-$  ( $10^{17.18}$ ) [37] all the sulphide should have been consumed to form  $\text{Cu}(\text{SH})_2^-/\text{Cu}_3\text{S}_3$  or a deposit of  $\text{Cu}_2\text{S}$  in the bottom of the cell, Fig. 5. This conversion was accelerated by magnetically stirring the solution at 10 Hz. The solution was filtered through Grade 1 filter paper with a pore size of 11  $\mu\text{m}$ , then a 0.2  $\mu\text{m}$  Acrodix syringe filter, and finally a 20 nm Whatman inorganic membrane filter. Since the size of  $\text{Cu}_3\text{S}_3$  clusters were expected to be in the range 100–200 nm [38], these clusters and any  $\text{Cu}_2\text{S}$  deposited particles (commonly microns in size, Fig. 5) would have been removed yielding a 0.1 mol/L NaCl solution containing only  $\text{Cu}(\text{SH})_2^-$  complexes. A clean Cu electrode was then placed in the filtered solution for 430 h (experiment 5). The electrode was subsequently removed and the surface and a FIB-cut cross section examined, Fig. 6. The electrode surface was covered with a non-uniformly distributed  $\text{Cu}_2\text{S}$  film, Fig. 6(a) and the FIB-cut cross section showed the Cu surface

to be roughened by corrosion and covered by a film 200 nm to 500 nm thick, confirming a corrosive interaction between the Cu and the Cu(SH)<sub>2</sub><sup>-</sup> complexes yielding Cu<sub>2</sub>S.

To consume all the SH<sup>-</sup> the following reaction would be required,  $2\text{Cu} + 2\text{Cu}(\text{SH})_2^- \rightarrow 2\text{Cu}_2\text{S} + 2\text{SH}^- + \text{H}_2$

with the excess SH<sup>-</sup> being subsequently consumed by further reaction with Cu to form Cu<sub>2</sub>S and H<sub>2</sub>. The need to oxidize additional Cu in order to produce Cu<sub>2</sub>S explains why no deposition was observed in the experiment with a Pt electrode (experiment 2).

The concern remained that, even though the mass and charge balance calculations indicated complete consumption of the SH<sup>-</sup> by the formation of Cu(SH)<sub>2</sub><sup>-</sup>/Cu<sub>3</sub>S<sub>3</sub>/Cu<sub>2</sub>S some SH<sup>-</sup> could remain adsorbed on the high surface area of the Cu<sub>2</sub>S deposit. To check for this possibility the deposit from experiment 4 was dried and then samples exposed to either Type I H<sub>2</sub>O or a 0.1 mol/L Na<sub>2</sub>SO<sub>4</sub> solution. After immersion of clean Cu electrodes in these solutions for 430 h (experiment 6) no visible corrosion occurred, Fig. 7, demonstrating that no SH<sup>-</sup> residue remained on the Cu<sub>2</sub>S deposits and confirming that all the available SH<sup>-</sup> had been consumed. That this observation demonstrated the complete sequestration of the available SH<sup>-</sup> is supported by our previous study which showed that even trace levels of SH<sup>-</sup> lead to observable Cu corrosion and Cu<sub>2</sub>S deposition [44].

#### 4. Conclusion

A galvanically-coupled experiment using pre-corroded and clean Cu electrodes in a 0.1 mol/L NaCl solution containing  $5 \times 10^{-4}$  mol/L SH<sup>-</sup> confirmed that Cu transport occurred between net anodic and net cathodic surface locations. This process was investigated in a sequence of experiments following the logic map outlined in Fig. 8.

ICP-MS, UV spectroscopy and MS demonstrated that the Cu species were present in solution and transported in the form of both solution soluble Cu complexes, predominantly Cu(SH)<sub>2</sub><sup>-</sup>, and Cu<sub>3</sub>S<sub>3</sub> clusters.

After stripping all the Cu complexes and clusters and deposited Cu<sub>2</sub>S particles from solution the absence of visible corrosion on a Cu specimen subsequently exposed to the Type I H<sub>2</sub>O or 0.1 mol/L Na<sub>2</sub>SO<sub>4</sub> solution confirmed all the available sulphide had been sequestered during the corrosion process.

#### Acknowledgements

This research was funded by Svensk Karnbranslehantering AB (Stockholm, Sweden), Posiva Oy (Olkiluoto, Finland) and the Nuclear Waste Management Organization (Toronto, Canada).

#### References

- [1] R.B. Bird, W.E. Stewart, E.N. Lightfoot, *Transport Phenomena*, 2nd ed., John Wiley & Sons, Inc., 2007.
- [2] B. Chopard, H.J. Hermann, T. Vicsek, Structure and growth mechanism of mineral dendrites, *Nature* 353 (1991) 409.
- [3] K.W. Burton, R.K.O. Nions, The timing of mineral growth across a regional metamorphic sequence, *Nature* 357 (1992) 235.
- [4] A. Baker, P.L. Smart, R.L. Edwards, D.A. Richards, Annual growth banding in a cave stalagmite, *Nature* 364 (1993) 518–520.
- [5] M.F. Hochella, S.K. Lower, P.A. Maurice, R.L. Penn, N. Sahai, D.L. Sparks, B.S. Twining, Nanominerals, mineral nanoparticles, and earth systems, *Science* 319 (2008) 1631–1635.
- [6] F.A. Bazzaz, R.W. Carlson, J.L. Harper, Contribution to reproductive effort by photosynthesis of flowers and fruits, *Nature* 279 (1979) 554–555.
- [7] S. Diaz, J.P. Grime, J. Harris, E. McPherson, Evidence of a feedback mechanism limiting plant response to elevated carbon dioxide, *Nature* 364 (1993) 616–617.
- [8] G.H. Brimhall, O.A. Chadwick, C.J. Lewis, W. Compston, I.S. Williams, K.J. Danti, W.E. Dietrich, M.E. Power, D. Hendricks, J. Bratt, Deformational mass transport and invasive processes in soil evolution, *Science* 255 (1992) 695–703.
- [9] B.K. Singh, R.D. Bardgett, P. Smith, D.S. Reay, Microorganisms and climate change: terrestrial feedbacks and mitigation options, *Nat. Rev. Microbiol.* 8 (2010) 779–790.
- [10] S. Wong, V. Kitaev, G.A. Ozin, Colloidal crystal films: advances in universality and perfection, *J. Am. Chem. Soc.* 125 (2003) 15589–15598.
- [11] J. Puthusser, S. Seefeld, N. Berry, M. Gibbs, M. Law, Colloidal iron pyrite (FeS<sub>2</sub>) nanocrystal inks for thin-film photovoltaics, *J. Am. Chem. Soc.* 133 (2010) 716–719.
- [12] J.G. McAlpin, Y. Surendranath, M. Dinca, T.A. Stich, S.A. Stoian, W.H. Casey, D.G. Nocera, R.D. Britt, EPR evidence for Co (IV) species produced during water oxidation at neutral pH, *J. Am. Chem. Soc.* 132 (2010) 6882–6883.
- [13] J. Chen, Z. Qin, T. Martino, D.W. Shoesmith, Non-uniform film growth and micro/macrogalvanic corrosion of copper in aqueous sulphide solutions containing chloride, *Corros. Sci.* 114 (2017) 72–78.
- [14] H. Xue, W. Sunda, Comparison of [Cu<sup>2+</sup>] measurements in lake water determined by ligand exchange and cathodic stripping voltammetry and by ion-selective electrode, *Environ. Sci. Technol.* 31 (1997) 1902–1909.
- [15] T.F. Rozan, M.E. Lassman, D.P. Ridge, G.W. Luther III, Evidence for multinuclear Fe, Cu and Zn molecular sulfide clusters in oxic river waters, *Nature* 406 (2000) 879–882.
- [16] S. Schneider, J.R. Ireland, M.C. Hersam, T. Marks, Copper (I) tert-butylthiolate clusters as single-source precursors for high-quality chalcocite thin films: film growth and microstructure control, *Chem. Mater.* 19 (11) (2007) 2780–2785.
- [17] J. Chen, Z. Qin, D.W. Shoesmith, Kinetics of corrosion film growth on copper in neutral chloride solutions containing small concentrations of sulfide, *J. Electrochem. Soc.* 157 (2010) C338–C345.
- [18] J. Chen, Z. Qin, D.W. Shoesmith, Long-term corrosion of copper in a dilute anaerobic sulfide solution, *Electrochim. Acta* 56 (2011) 7854–7861.
- [19] J. Chen, Z. Qin, D.W. Shoesmith, Rate controlling reactions for copper corrosion in anaerobic aqueous sulphide solutions, *Corros. Sci. Eng. Tech.* 46 (2011) 138–141.
- [20] J. Chen, Z. Qin, L. Wu, J.J. Noël, D.W. Shoesmith, The influence of sulphide transport on the growth and properties of copper sulphide films on copper, *Corros. Sci.* 87 (2014) 233–238.
- [21] B.C. Syrett, The mechanism of accelerated corrosion of copper-nickel alloys in sulphide-polluted seawater, *Corros. Sci.* 21 (1981) 187–209.
- [22] S.R. De Sanchez, D.J. Schiffrin, The flow corrosion mechanism of copper base alloys in sea water in the presence of sulphide contamination, *Corros. Sci.* 22 (1982) 585–607.
- [23] L.E. Eiselstein, B.C. Syrett, S.S. Wing, R.D. Caligiuri, The accelerated corrosion of Cu-Ni alloys in sulphide-polluted seawater: mechanism no. 2, *Corros. Sci.* 23 (3) (1983) 223–239.
- [24] S.R. De Sanchez, D.J. Schiffrin, The use of high speed rotating disc electrodes for the study of erosion-corrosion of copper base alloys in sea water, *Corros. Sci.* 28 (1988) 141–151.
- [25] A.M. Beccaria, G. Poggi, P. Traverso, M. Ghiazza, A study of the de-alloying of 70Cu-30Ni commercial alloy in sulphide polluted and unpolluted sea water, *Corros. Sci.* 32 (11) (1991) 1263–1275.
- [26] J.N. Al-Hajji, M.R. Reda, The corrosion of copper-nickel alloys in sulfide-polluted seawater: the effect of sulfide concentration, *Corros. Sci.* 34 (1993) 163–177.
- [27] T.T.M. Tran, C. Fiaud, E.M.M. Sutter, A. Villanova, The atmospheric corrosion of copper by hydrogen sulphide in underground conditions, *Corros. Sci.* 45 (12) (2003) 2787–2802.
- [28] K. Rahmouni, M. Keddad, A. Shiri, H. Takenouti, Corrosion of copper in 3% NaCl solution polluted by sulphide ions, *Corros. Sci.* 47 (12) (2005) 3249–3266.
- [29] D.W. Shoesmith, Assessing the corrosion performance of high-level nuclear waste containers, *Corrosion* 62 (2006) 703–722.
- [30] D. Féron, D. Cruset, J.-M. Gras, Corrosion issues in nuclear waste disposal, *J. Nucl. Mater.* 378 (2008) 16–23.
- [31] F. King, M. Kolar, M. Vahanen, C. Lilja, Modelling long term corrosion behaviour of copper canisters in KBS-3 repository, *Corros. Eng. Sci. Tech.* 46 (2011) 217–222.
- [32] D.D. Wagman, W.H. Evans, V.B. Parker, R.H. Schumm, I. Halow, S.M. Bailey, K.L. Churney, R.L. Nuttall, The NBS tables of chemical thermodynamic properties, *J. Phys. Chem. Ref. Data* 2 (Supplement No. 2) (1982).
- [33] J.M. Smith, J.C. Wren, M. Odziemkowski, D.W. Shoesmith, The electrochemical response of preoxidized copper in aqueous sulfide solutions, *J. Electrochem. Soc.* 154 (8) (2007) C431–C438.
- [34] E. Protopopoff, P. Marcus, Potential-pH diagrams for sulfur and hydroxyl adsorbed on copper surfaces in water containing sulfides, sulfites or thiosulfates, *Corros. Sci.* 45 (2003) 1191–1201.
- [35] H.M. Hollmark, P.G. Keech, J.R. Vegelius, L. Werme, L.-C. Duda, X-ray absorption spectroscopy of electrochemically oxidized Cu exposed to Na<sub>2</sub>S, *Corros. Sci.* 54 (2012) 85–89.
- [36] E.M. Khairy, N.A. Darwish, Studies on copper-semiconducting layer-electrolyte systems—I. Galvanostatic anodic polarization of Cu/Cu<sub>2</sub>S/S<sup>2-</sup> applying stationary and rectangular pulse techniques, *Corros. Sci.* 13 (1973) 149–164.
- [37] D.A. Crerar, H.L. Barnes, Ore solution chemistry; V, solubilities of chalcopyrite and chalcocite assemblages in hydrothermal solution at 200 degrees to 350 degrees C, *Econ. Geol.* 71 (1976) 772–794.
- [38] B.W. Mountain, T.M. Steward, The hydrosulphide/sulphide complexes of copper (I): Experimental determination of stoichiometry and stability at 22 °C and reassessment of high temperature data, *Geochim. Cosmochim. Acta* 63 (1999) 11–29.
- [39] Z.G. Xiao, J. Brose, S. Schimo, S.M. Ackland, S.L. Fontaine, A.G. Wedd, Unification of the copper (I) binding affinities of the metallo-chaperones Atx1, Atox1, and related proteins detection probes and affinity standards, *J. Biol. Chem.* 286 (2011) 11047–11055.
- [40] Z. Xiao, F. Loughlin, G.N. George, G.J. Howlett, A.G. Wedd, C-terminal domain of the membrane copper transporter Ctr1 from *Saccharomyces cerevisiae* binds four Cu(I) ions as a cuprous-thiolate polynuclear cluster: sub-femtomolar Cu(I) affinity of three proteins involved in copper trafficking, *J. Am. Chem. Soc.* 126 (2004) 3081–3090.
- [41] B. Zak, Simple procedure for the single sample determination of serum copper and iron, *Clin. Chim. Acta* 3 (1958) 328–334.
- [42] J. Crousier, L. Pardessus, J.P. Crousier, Voltammetry study of copper in chloride solution, *Electrochim. Acta* 33 (1988) 1039–1042.
- [43] D.R. Lide, *CRC Handbook of Chemistry and Physics*, CRC press, 2003–2004.
- [44] T. Standish, J. Chen, R. Jacklin, P. Jakupi, S. Ramamurthy, D. Zagidulin, D.W. Shoesmith, Corrosion of copper-coated steel high level nuclear waste containers under permanent disposal conditions, *Electrochim. Acta* 211 (2016) 331–342.